# A Solution Approach to Component Dynamics of A/B Miscible Blends. 1. Tube Dilation, Reptation, and Segmental Friction of Polymer A

**Xiaoping Yang, Shi-Qing Wang,* and H. Ishida**

*Department of Macromolecular Science, Case Western Reserve University, Cleveland, Ohio 44106-7202*

*Received November 17, 1998; Revised Manuscript Received February 17, 1999*

ABSTRACT: A model solution system of 1,4-polybutadiene in oligomeric butadiene of high vinyl content is studied to show how polymer friction dynamics depend explicitly on the solvent dynamics and are approximately determined by the overall glass transition temperatures of the solutions as a function of concentration (i.e., weight fraction $\phi$) and temperature $T$. Among the most striking findings are the invariance of the overall molecular relaxation time with $\phi$ from $\phi = 1.0$ to 0.3 at a special temperature $T_0$. Below $T_0$, the solutions possess longer reptation times than that of the pure PBD melt. Moreover, through oscillatory shear measurements of linear viscoelasticity, the scaling of the tube dilation with $\phi$ is found rheologically as $a \propto \phi^{-2/3}$, which agrees with the previous neutron spin echo studies. Since viscoelastic properties of the entangled solutions reveal dynamics associated with the polymeric component, a general methodology is established here based on the present model system for characterization of component dynamics in miscible polymer blends.

## Introduction

A reliable description of dynamics in polymer mixtures is the first step toward establishing a basic understanding of blends in processing. Ordinarily, various components of a blend may have a comparable level of chain entanglement when examined as pure substances. Upon blending two such components to form a binary mixture, we attain either a uniform one-phase material or a heterogeneous material comprising of two phases, each of which is a miscible blend. Since both components in a miscible blend contribute to the overall viscoelastic and rheological properties, it is not simple to distinguish dynamics due to component A from those due to component B. On the other hand, this distinction is necessary if we would like to understand the origin of the reported breakdown of the time−temperature superposition principle in miscible blends.[1−3] In particular, we would like to be able to reveal how each component's dynamics depend on temperature as a function of the blend composition $\phi$ (i.e., the weight or volume fraction of component A).

Several experimental techniques have been proposed to accomplish the task of quantitatively differentiating component dynamics that are encountered in a miscible blend. Tracer diffusion measurements were carried out in an attempt to extract information about the segmental friction coefficients $\zeta_A(\phi,T)$ and $\zeta_B(\phi,T)$ of the respective components A and B as a function of $\phi$ at an equal distance from the effective glass transition temperature $T_g(\phi)$ of the blends,[4−7] where $\zeta_A$ and $\zeta_B$ might be related to the tracer diffusion constants $D_A$ and $D_B$. This was done by allowing interdiffusion between a blend at a given composition $\phi$ and *pure* deuterated films of components A and B, respectively, and by fitting a calculated concentration profile containing $D_A$ and $D_B$, respectively, to the experimental one measured using forward recoil spectrometry. The two polymers (components) under study were polystyrene and poly(xylenyl ether),[4] which is also called poly(phenylene oxide). Since their glass transition temperatures $T_g$ (= 100 and 217 °C for PS and PXE, respectively) are so different, the interdiffusion process was much slower when involving a pure d-PXE film in contact with a blend in comparison to the situation involving a pure d-PS film in contact with the same blend. As a result, $\zeta_{PXE}$ was found to be vastly greater than $\zeta_{PS}$ by 2−4 orders of magnitude at various values of $\phi$. Similar results were reported subsequently using the same protocol.[5−7] For instance, $\zeta_{PS}$ was found to show a strong maximum as a function of the blend composition $\phi$ at an equal distance from the effective blend glass transition temperature $T_g(\phi)$.[5] These results appear to be controversial and at odds with the more recent forced Rayleigh scattering studies on a different system.[8]

A second experimental technique involves a combination of rheo-optical and rheological measurements. To obtain $\zeta_A$ and $\zeta_B$ as a function of temperature at different values of $\phi$,[3,9] it was assumed that the overall viscoelasticity, e.g., the complex modulus $G^*_{blend}$, of the blend can be *linearly decomposed* into the hypothetical $G^*_A$ and $G^*_B$ of the components A and B, both of which are unknown. By applying the stress-optical rule and assuming a similar linear superposition for the complex birefringence, Arendt et al.[3,9] established two equations for the two unknown complex moduli $G^*_A$ and $G^*_B$, respectively. From $G^*_{A,B}$, $\zeta_{A,B}$ was respectively evaluated according to the reptation theory.

A third method is that of the forced Rayleigh scattering.[8] This technique directly evaluates the self-diffusion process of the labeled chains in a blend. As long as the labeled chains have nearly the same glass transition temperatures as those of the unlabeled components, the FRS measurements should yield relatively reliable results.

Polymer solutions, a special case of miscible polymer blends, have been well studied for their equilibrium and dynamic properties. As far as chain entanglement and reptation dynamics are concerned, one effect of diluting a strongly entangled melt is to dilate the tube diameter

* Corresponding author. E-mail sxw13@po.cwru.edu.

10.1021/ma981778w CCC: $18.00 
Published on Web 03/24/1999

*a* within which each chain is confined according to the tube model of Edwards.[10] A more interesting effect of incorporating oligomeric chains or solvent of species B (e.g., of different $T_g$) into a polymeric melt of species A amounts to altering the local friction dynamics. Usually the selected solvent has such fast dynamics due to its extraordinarily low crystallization point and glass transition temperature that the chain dynamics are governed by those of the solvent. As a result, the segmental friction coefficient $\zeta$ hardly has any concentration dependence at various temperatures. Actually, molecular theories nearly never explicitly consider the concentration dependence of $\zeta$.[10] Here we are motivated to consider solutions where the "solvent" has a much higher glass transition temperature than that of the polymer. Incorporation of the polymer leads to "plasticization" of the solvent. As a result, the segmental friction coefficient $\zeta_A(\phi,T)$ of A chains develops explicit concentration dependence at various temperatures. By studying viscoelastic properties of *entangled* solutions, made of polymeric A in oligomeric B and polymeric B in oligomeric A, respectively, we can explore the component dynamics of a corresponding polymer blend of A and B species. For entangled solutions, the viscoelastic characteristics are dominated by the polymeric component. Consequently, the time−temperature superposition principle is expected to apply for the solutions even when it breaks down for the polymer blend of A and B.

One purpose of this paper is to introduce and illustrate a general rheological approach for studying polymer blend dynamics based on solution samples made from the components of the blend. This new method does not require any chemical modification such as deuteration and should be applicable to any miscible polymer blends. A second purpose of this paper is to report an intriguing example of entangled polymer solution dynamics showing *invariance* of the terminal molecular relaxation time $\tau_d$ (i.e., the reptation time for disentanglement) with the concentration $\phi$ at a specific temperature. In this case, the zero-shear solution viscosity $\eta_0$ decreases with $\phi$, yet $\tau_d$ is constant, where the lower $\eta_0$ at smaller $\phi$ is due entirely to decreasing of the elastic plateau modulus $G_N^0(\phi)$ with lowering $\phi$. Furthermore, this work represents a first *rheological* determination of the tube diameter scaling with $\phi$ throughout the concentration range and confirms a scaling relation between the plateau modulus and tube diameter. Finally, the present results illustrate that the solution dynamics, depicted by the reptation time $\tau_d$ and the segmental friction coefficient $\zeta(\phi,T)$, can be approximately described by the WLF relation based on the solution's effective glass transition temperature $T_g(\phi)$.

## Experimental Section

**Materials.** Our model solutions consist of linear 1,4-polybutadiene (PBD) synthesized and analyzed with GPC and NMR in Dr. Adel Halasa's laboratory in the Goodyear Research Center and oligomeric butadiene (oBD) of different chemical compositions purchased from Aldrich. Table 1 shows the 1,4-PBD and oBD characteristics. Since the critical molecular weight for chain entanglement, $M_e$, is less than 2000, the two PBD are highly entangled. Solutions of two 1,4-PBD in two kinds of oBD are respectively prepared at weight fractions $\phi$ = 0.75, 0.5, and 0.3. It is worth noting that oBD1 contains 60% unsaturation.

**Apparatus.** Linear viscoelastic properties of the PBD solutions are measured by a dynamic mechanical spectrometer (Rheometrics RMS-800) at frequencies ranging from 0.1 to 100 rad/s and temperatures from 80 to −80 °C. The spectrometer is equipped with a 200−2000 g cm dual range and a force rebalance transducer, and oscillatory shear measurements are carried out using 25 mm diameter parallel plates. To measure the overall glass transition temperature $T_g$ of the 1,4-PBD solutions and melts, a modulated DSC (DSC 2920 from TA instruments) is employed.

**Table 1. Characteristics of PBD and Oligomeric BD**

| | $M_w$ ($\times10^{-3}$) | $M_n$ ($\times10^{-3}$) | vinyl (%) | cis-1,4 (%) | trans-1,4 (%) | $T_g$ (°C) |
|---|---|---|---|---|---|---|
| PBD1 | 437 | 270 | 10 | 35 | 55 | −94 |
| PBD2 | 244 | 205 | 10 | 35 | 55 | −95 |
| oBD1 | | 1.0 | 45 | 5 | 10 | −51 |
| oBD2 | | 1.5 | 25 | 35 | 40 | −89 |

## Theoretical Analysis

Chain dynamics can be studied by applying the well-established tube reptation model of de Gennes−Doi−Edwards[10,11] for linear viscoelastic properties of entangled polymers. The following simple generalizations of the original reptation theory can be made to delineate solution dynamics: (a) the tube diameter $a(\phi)$ is concentration-dependent, thanks to swelling of the tube by the low molar mass "solvent"; (b) the Rouse segmental friction coefficient $\zeta(\phi,T)$ is a function of concentration due to the concentration dependence of the glass transition temperature $T_g(\phi)$; (c) the plateau modulus $G_N^0(\phi)$ is proportional to the polymer volume fraction $\phi$ and inversely proportional to the square of the tube diameter:

$$G_N^0(\phi) \propto \phi/[a(\phi)]^2 \tag{1}$$

which follows directly from (7.43) of Doi and Edwards[10] by replacing the segment density $c$ with the polymer volume fraction $\phi$. A similar result has been derived by Graessley and Edwards.[12] The chain relaxation time $\tau_d$ for disentanglement has the following explicit $\phi$ dependence for a chain of length $N$

$$\tau_d \propto \frac{\zeta(\phi,T)N^3}{k_BT[a(\phi)]^2} \tag{2}$$

which preserves the original scaling $N^3$. The friction coefficient $\zeta(\phi,T)$ in (2) dominates the temperature dependence and also exhibits concentration dependence stemming from $T_g(\phi)$, both according to a WLF relation[13]

$$\log\left[\frac{\zeta(\phi,T)}{\zeta_g(\phi)}\right] = -\frac{c_1[T - T_g(\phi)]}{c_2 + T - T_g(\phi)} \tag{3}$$

with $c_1$ and $c_2$ being the WLF constants and $\zeta_g(\phi)$ the friction coefficient at $T_g(\phi)$. The case of the pure melt is included in (3), corresponding to setting $\phi = 1.0$ and labeling $c_1$, $c_2$, and $T_g$ with a subscript zero. This WLF equation can be also written down with respect to a reference temperature $T_0$ rather than $T_g$. With respect to $T_0$, we have a different set of the WLF constants $c_{01}$ and $c_{02}$. $c_1$ and $c_2$ can be expressed in terms of ($T_0 - T_g$), $c_{01}$, and $c_{02}$ by solving the following equation

$$-\frac{c_{01}(T - T_0)}{c_{02} + T - T_0} = -\frac{c_1(T - T_g)}{c_2 + T - T_g} + \frac{c_1(T_0 - T_g)}{c_2 + T_0 - T_g} \tag{4a}$$

The solutions

$$c_2 = c_{02} - (T_0 - T_g) \quad \text{and} \quad c_1 = c_{01}c_{02}/c_2 \tag{4b}$$

which are the same as given previously,[13] are obtained by solving (4a) for any two temperatures $T$ and $T'$.

It is also useful to introduce the tube constraint time $\tau_e$ corresponding to segmental motion on the length scale of the tube diameter $a(\phi)$[10]

$$\tau_e \propto \zeta(\phi,T)[a(\phi)]^4/k_BT \tag{5}$$

The reciprocal of $\tau_e$ defines the onset of the rubber–glass transition or Rouse region in the frequency domain. By taking the ratio $\tau_d/\tau_e$ to represent the width of the rubbery plateau, we obtain the tube diameter $a$ from oscillatory shear measurements as

$$a(\phi) \propto [\tau_d/\tau_e]^{-1/6} \tag{6}$$

which follows from the explicit expressions 2 and 5 for the two time scales. If $a(\phi)$ dilates with the concentration $\phi$ as

$$a(\phi) = a_0\phi^{-\theta} \tag{7a}$$

where hereafter the subscript zero denotes quantities of the pure polymer melt, then (1) gives an explicit dependence of the plateau modulus $G_N^0(\phi)$ on $\phi$

$$G_N^0(\phi) = G_N^0\phi^{1+2\theta} \tag{7b}$$

where $G_N^0$ is that of the pure melt. In the semidilute regime, a de Gennes type scaling argument based on the blob concept yields $\theta = 2/3$ for $\Theta$ solvents and $\theta = 3/4$ for good solvents.[14]

The preceding analysis indicates that the tube dilation as a function of concentration can be determined by evaluating the ratio of time scales from oscillatory shear measurements according to (6). The concentration dependence of the friction coefficient $\zeta(\phi,T)$ can be obtained from (2) by measuring $\tau_d(\phi,T)$ and inserting $a(\phi)$ derived from (6). In other words, it is shown that from an oscillatory shear experiment covering the terminal, plateau, and rubber–glass transition regions we can approximately determine the concentration dependence of $a(\phi)$, $G_N^0(\phi)$, and $\zeta(\phi,T)$. In the present paper, we would like to explore how these quantities change as a pure polybutadiene melt is diluted down to $\phi = 0.3$ where the solution is still highly entangled.

## Results and Discussion

**Scaling of Tube Diameter and Plateau Modulus.** Oscillatory shear measurements on PBD1 are first carried out at 10 different temperatures—80, 40, 20, 0, −15, −30, −45, −60, −75, and −80 °C—in order to obtain the complex modulus $G^*$ over all three regions (terminal, plateau, and Rouse) spanning nearly 10 decades using the time–temperature superposition (TTS) principle. Then similar measurements at respective temperatures 80, 40, 0, −30, and −60 °C were performed on solutions made of PBD1 in oBD1 with composition $\phi = 0.75$ and 0.5 and at 80, 40, 0, and −30 °C for $\phi = 0.3$. Again the TTS is applied to obtain the master curves for $G^*$ as a function of the oscillation frequency $\omega$. As asserted in the Introduction, the TTS principle should hold for these *entangled* solutions even though blends of *poly*butadienes of low and high vinyl contents are known to violate it.[2] Figure 1 shows the loss modulus for the three solutions obtained on the basis of the TTS. Existence of these master curves suggests that the TTS principle is applicable for the entangled solutions. To show more clearly the power of $^1/_2$ in the high-frequency region and the change of the negative slope with concentration (or extent of chain entanglement), the data in Figure 1 have been vertically shifted to overlap in the terminal region.

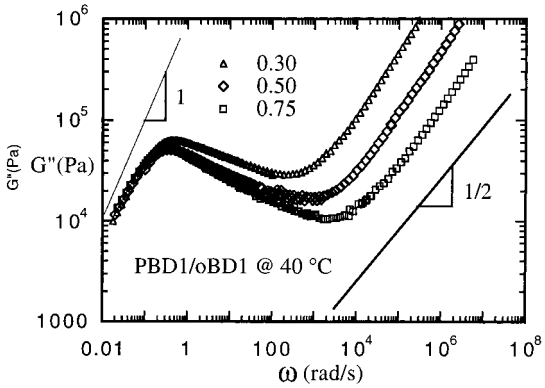


**Figure 1.** Loss modulus $G''$ of three PBD1 solutions obtained using the time–temperature superposition at the reference temperature of 40 °C.

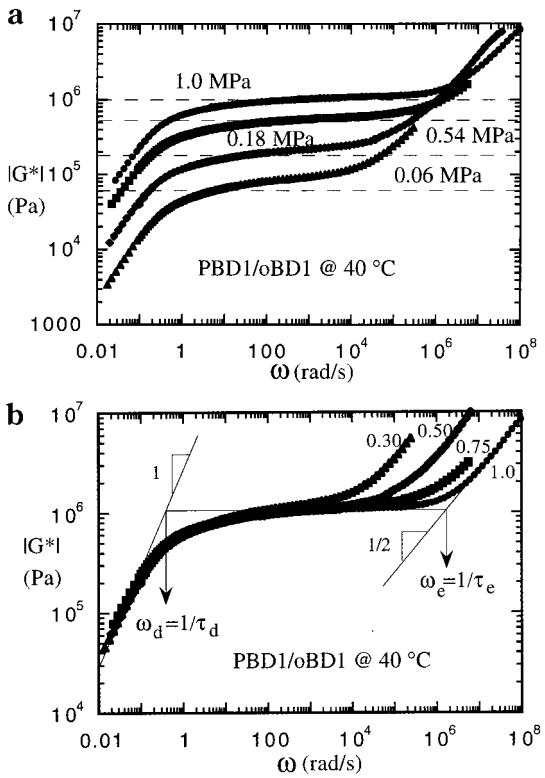


**Figure 2.** (a) Complex modulus $|G^*|$ of the pure PBD1 and its three solutions at 40 °C, where the dashed lines show the predicted values of the plateau modulus. (b) Complex modulus $|G^*|$ of the same four samples obtained by vertical shifting of (a) to bring overlapping in the terminal and plateau regions.

Figure 2a shows the complex moduli $G^*$ as a function of the oscillation frequency $\omega$ at $T = 40$ °C for the pure PBD1 as well the PBD1/oBD1 solutions. The comparison between the different samples can be made more transparent as shown in Figure 2b by simply vertically

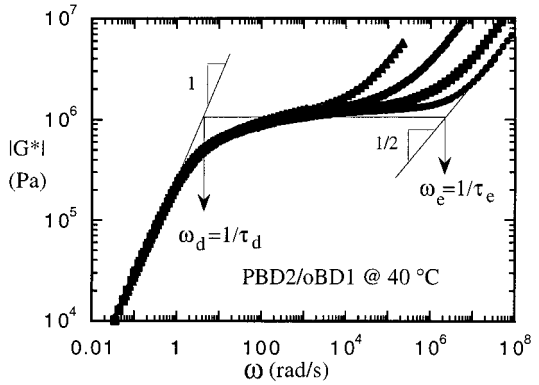


**Figure 3.** Complex modulus $|G^*|$ of the pure PBD2 and its three solutions at 40 °C after the vertical shift.

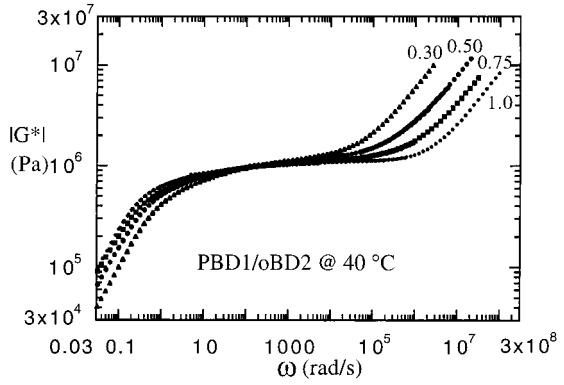


**Figure 4.** Complex modulus $|G^*|$ of the pure PBD1 and its three solutions in oBD2 at 40 °C after the same vertical shift that is employed to obtain Figures 2b and 3.

shifting the all solution curves in Figure 2a upward until their elastic plateau moduli overlap with that of the pure melt. It is seen from Figure 2b that the onset of the plateau approximately occurs at the same frequency, indicating almost identical terminal relaxation times $\tau_d$ for all the four samples. This phenomenon remains essentially true for PBD2 and its solutions as shown in Figure 3, where 80, 40, 0, −25, −40, −65, −75, and −80 °C are the eight temperatures used to carry out the oscillatory shear measurements for the pure PBD2, six temperatures 80, 40, 0, −30, −60, and −70 °C for $\phi = 0.75$, five temperatures 80, 40, 0, −30, and −60 °C for $\phi = 0.50$, and four temperatures 80, 40, 0, and −30 °C for $\phi = 0.30$. The horizontal lines in Figures 2b and 3 are drawn at $G_N^0 = 1.0$ MPa, which is the well-known value for 1,4-PBD melts.

The surprising invariance of the reptation time $\tau_d$ with concentration $\phi$ suggests, according to (2), that at 40 °C the friction coefficient $\zeta(\phi,T)$ of PBD1 segments increases with $\phi$ in the same way as the tube diameter $[a(\phi)]^2$ changes with $\phi$. In contrast, the onset of the Rouse region, where the time scale $\tau_e$ of (5) is identified, varies more strongly with $\phi$. Since $\zeta$ cancels $[a(\phi)]^2$ in (5) at this temperature of 40 °C, $\tau_e$ actually varies with $\phi$ as $[a(\phi)]^2$ according to (5).

In contrast to the effect of oBD1 on the polymer dynamics that enhances the segmental friction coefficient $\zeta(\phi,T)$, PBD1 in oBD2 shows the more familiar behavior where $\zeta(\phi,T)$ is little affected by the diluent oBD2. As a consequence, the polymer dynamics speed up with dilution due to the common tube dilation effect. In other words, the reptation time given in (2) decreases with decreasing $\phi$. Figure 4 shows that the flow curves of the solutions indeed move to the right-hand side with respect to that of the pure PBD1 melt. To obtain Figure 4, measurements are carried at 80, 40, 0, −30, −60, and −75 °C for the solution of $\phi = 0.75$; at 80, 40, 0, −30, −60, and −70 °C for $\phi = 0.5$; and at 80, 40, 0, −30, and −60 °C for $\phi = 0.3$. The vertical shifts in Figure 4 are identical to those made for Figures 2b and 3. In other words, the elastic plateau moduli of these PBD1/oBD2 solutions are the same as those of the PBD1/oBD1 and PBD2/oBD1 solutions as illustrated in Figure 2a for the PBD1/oBD1 solution.

It is straightforward to describe how $a(\phi)$ scales with $\phi$ by calculating the time ratio given in (6) from Figures 2b, 3, and 4. Normalizing the tube diameter $a(\phi)$ of the solution with $a_0$ of the pure PBD, we show in Figure 5a that $a(\phi)$ accurately scales with $\phi$ with a familiar exponent of −2/3 for all three solutions, which has

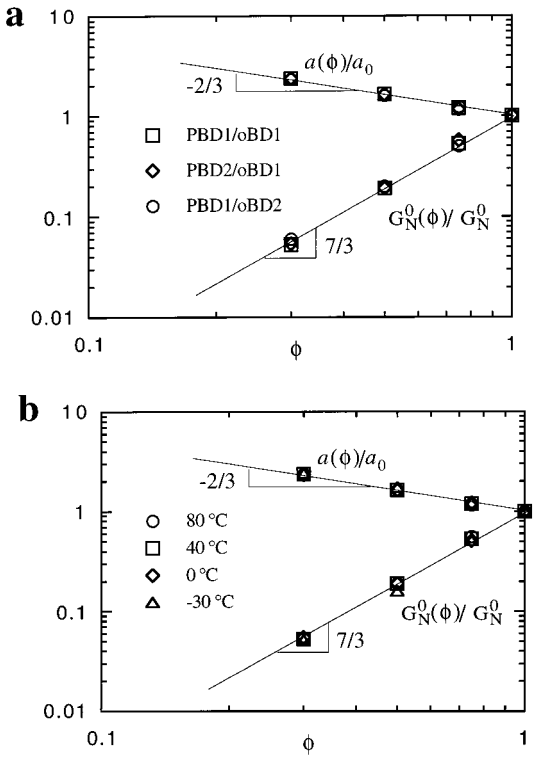


**Figure 5.** (a) Normalized tube diameter $a(\phi)/a_0$ and plateau modulus $G_N^0(\phi)/G_N^0 = \phi[a_0/a(\phi)]^2$ as a function of the weight fraction (i.e., concentration) $\phi$ for three different solutions at 40 °C, where the straight lines with slopes −2/3 and 7/3 are not the fit to the data but guide to the eye. (b) Scaling of $a/a_0$ and $G_N^0/G_N^0(0)$ with $\phi$ at four temperatures.

theoretically been argued to exist only in semidilute solutions[14] and experimentally been determined using neutron spin echo measurements.[15] According to (7b), we predict that the elastic plateau modulus of the solutions scales with $\phi$ as $G_N^0(\phi)/G_N^0 = \phi^{7/3}$, where $\theta = 2/3$. This prediction agrees rather well with the actual experimental data as shown in Figure 2a and with a previous report,[16] showing internal consistency of the reptation theory. Since the tube dilation does not depend on the segmental friction and reptation dynamics, the scaling of $a(\phi)/a_0 = \phi^{-\theta}$ holds true independently of molecular weight and vinyl content of the "solvent", as shown in Figure 5a. This static scaling is not expected to depend on temperature. Indeed, Figure 5b, obtained from the master curves of PBD1 at four different temperatures, confirms the speculation.

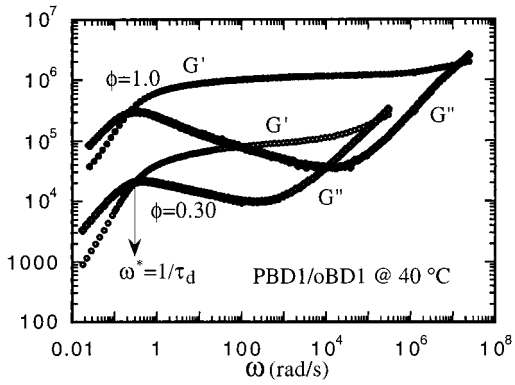


**Figure 6.** Storage and loss moduli $G'$ and $G''$ of the pure PBD1 and its 30% solution at 40 °C, showing the crossover frequency, where the smooth master curves indicate the validity of the time−temperature superposition.

**Reptation Time as a Function of Temperature, Molecular Weight, and Vinyl Content.** An explicit evaluation of $\tau_d$ from the oscillatory shear measurements is illustrated in Figure 6, as the reciprocal of the intersecting frequency $\omega^*$ where $G'(\omega^*) = G''(\omega^*)$. Reptation theory of Doi and Edwards[10] asserts that $\tau_d = 1/\omega^*$ is the disentanglement relaxation time for monodisperse polymers. $\omega^*$ in Figure 2b is numerically very close to $\omega_d = 1/\tau_d$ defined in Figures 2b and 3. For the pure PBD1, $\tau_{d0}$ is found to be 4.7 s, and the solution of $\phi = 0.3$ has $\tau_d(\phi) = 3.7$ s at 40 °C. Figure 6 further shows that the time−temperature superposition is valid for a highly entangled solution, in agreement with the conclusion made from Figure 1. The reptation time $\tau_d$ could also be evaluated for monodisperse samples from the zero-shear viscosity $\eta_0$ and the elastic plateau modulus $G_N^0$ according to the formula for $\eta_0$ from the classical reptation theory:[10] $\eta_0 = (\pi^2/12)G_N^0\tau_d$. We find reasonable agreement among the values of $\tau_d$ obtained in both ways, implying that the reptation theory is quantitatively accurate for linear viscoelastic properties of entangled polymers. Since PBD1 is not sufficiently monodisperse, a rigorous investigation of the relation between $\omega^*$ amd $\tau_d$ is not pursued here.

Following the method described in the preceding paragraph, we obtain $\tau_d(\phi,T) = 1/\omega^*$ of all eight samples made of PBD1 and PBD2 at different temperatures from the special temperature of 40 °C down to −30 °C as shown in Figures 7a,b. To understand the behavior exhibited by these samples, we need to know how the diluent, i.e., oBD1 of higher $T_g$, modifies the overall glass transition temperature $T_g(\phi)$. Differential scanning calorimetry has been carried out to obtain Figure 8 for the effective $T_g(\phi)$ as a function of $\phi$ for both oligomeric solvents. We see that the PBD1/oBD1 solutions have substantially higher $T_g(\phi)$ at a lower $\phi$. Consequently, the friction coefficient $\zeta(\phi,T)$ of a lower $\phi$ is closer to its value $\zeta_g(\phi)$ at the glass transition and thus larger than that of the pure PBD because the distance $[T - T_g(\phi)]$ in (3) is smaller. This effect cancels the effect of tube dilation at 40 °C and causes the reptation time $\tau_d$ of (2) not to decrease with lowering $\phi$ at $T < 40$ °C. At lower temperatures, the slowing down of the segmental dynamics by the solvent of high-vinyl oligomeric butadiene overwhelms the speeding up of the reptation dynamics by the solvent dilation of the tube. As a result, the solutions possess longer reptation times than that of the pure melt for $T < 40$ °C.

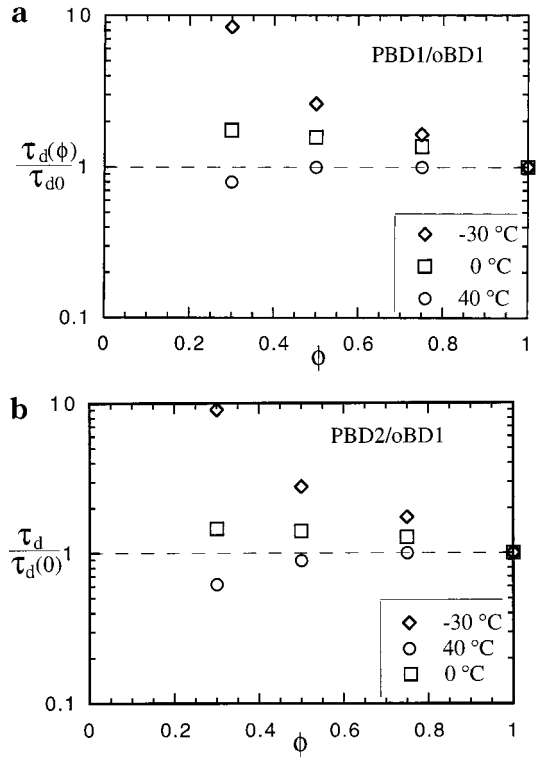


**Figure 7.** (a) Reptation time $\tau_d(\phi)$ of the solution as a function of $\phi$, normalized by that of the pure PBD1, $\tau_{d0}$, at three temperatures. (b) Reptation time $\tau_d(\phi)$ of the solution relative to $\tau_{d0}$ of the pure PBD2 at three temperatures.

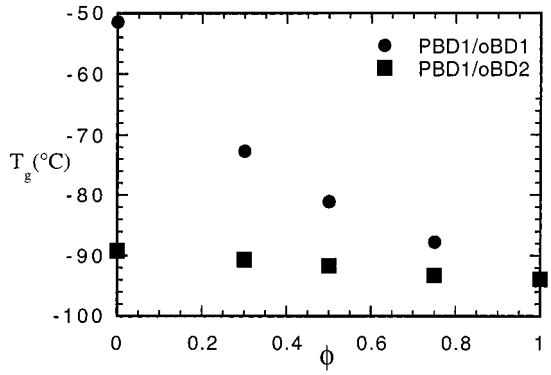


**Figure 8.** Effective glass transition temperatures $T_g(\phi)$ of the two solutions as a function of composition $\phi$ as determined by DSC.

At higher temperatures, i.e., sufficiently away from the glass transition temperatures, we see a weaker effect of oBD1 to slow down the PBD1 dynamics through the friction coefficient's dependence on $T_g(\phi)$ according to (3). Figure 9 shows that $\tau_d(\phi,T)$ of both PBD1/oBD1 and PBD2/oBD1 solution actually decreases with lowering $\phi$ at 80 °C. Since $\tau_d(\phi,T)$ approximately scales as $\phi^{2/3}$ as shown in Figure 9, we can infer from (2) and $a(\phi) \propto \phi^{-2/3}$ that $\zeta(\phi,T) \propto a(\phi)$ at $T = 80$ °C. This is indeed the case as shown in Figure 10. Figure 9 further elucidates that the friction coefficient $\zeta(\phi,T)$ and $\tau_d(\phi,T)/\tau_{d0}(T)$ of the PBD1/oBD2 solution appear to have $\phi$ dependence at both temperatures similar to that of the PBD1/oBD1 and PBD2/oBD1 solutions at 80 °C. Since the effective glass transition temperature of PBD1/oBD2 is nearly the same as that of the pure PBD1 as shown in Figure 8, the ratio $\tau_d(\phi,T)/\tau_{d0}(T)$ does not so sensitively depend on temperature $T$ as indicated by the overlapping of squares and diamonds in Figure 9.

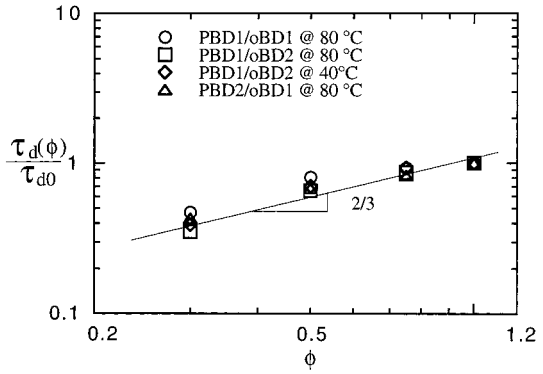


**Figure 9.** Reptation time $\tau_d(\phi)$ of the three solutions normalized by $\tau_{d0}$ of the pure melts at 40 and 80 °C, respectively.

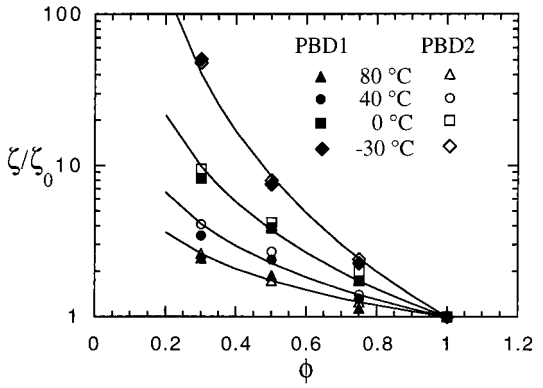


**Figure 10.** Ratio of segmental friction coefficient $\zeta$ of the solution to $\zeta_0$ of the pure PBD1 at four temperatures.

**Friction Coefficient and Its WLF-like Temperature Dependence.** Polymer dynamics of multicomponent systems depend explicitly on the frictional interaction between segments of various components. Specifically, the reptation time for disentanglement $\tau_d$ is directly proportional to the segmental friction coefficient $\zeta(\phi,T)$ that is the origin of the strong WLF-like temperature dependence. When the glass transition temperature $T_g$ of component A is widely different from that of component B, $\zeta_{A,B}(\phi,T)$ associated with components A and B may develop strong composition dependence. For a given $\phi$ and $T$, $\zeta_A$ is not expected to be greatly different from $\zeta_B$ in a miscible system (either solution or blend) since both components experience the same effective glass transition temperature $T_g(\phi)$. Here we provide a first example to show that $\zeta_A$ and $\zeta_B$ associated with a polymer blend of components A and B can be separately evaluated as a function of $\phi$ and $T$ by studying the corresponding solution properties of polymeric A in oligomeric B and polymeric B in oligomeric A.

In the present paper, we show how $\zeta$ of 1,4-PBD in oligomeric butadiene of high vinyl content (object system) can be obtained at different compositions and temperatures. In the near future we will carry out a similar investigation on the "mirror" solutions of high-vinyl PBD in oligomeric 1,4-butadiene. It is well-known that the segmental friction coefficient $\zeta$ for an oligomer may depend on its molecular weight due to the molecular weight dependence of its glass transition temperature. Thus, in preparation of the mirror systems to be studied in paper 2, two possibilities arise, assuming the criterion for a mirror solution is to match the glass transition temperature of the "object" and "mirror" solutions. In case a, we will use an oligomer of 1,4-BD of equal vinyl content (10%) that may have a $T_g$ slightly different from that of PBD1. This means the composition of the "object" and "mirror" systems will have to be slightly different. In case b, we will have an oligomeric 1,4-BD of slightly different vinyl content while keeping the composition the same. These subtleties are not expected to derail our basic objective of evaluating $\zeta_A$ and $\zeta_B$ in sufficiently similar dynamic environments.

**Table 2. WLF Constants of PBD1 and Solutions at $T_0$ and $T_g(\phi)$**

| $\phi$ | $T_0$ (°C) | $c_{01}$ | $c_{02}$ | $T_g$ (°C) | $c_1$ | $c_2$ | $T_g'$ (°C) |
|---|---|---|---|---|---|---|---|
| 1.0 | 39 | 3.22 | 185.8 | −94 | 11.4 | 52.8 | −94 |
| 0.75 | 38 | 3.55 | 175.7 | −87.8 | 12.5 | 49.9 | −92 |
| 0.5 | 39 | 3.76 | 171.3 | −81 | 12.6 | 51.1 | −84 |
| 0.3 | 39 | 3.76 | 157.5 | −72.7 | 13.1 | 45.3 | −73.5 |

According to (2), $\zeta(\phi,T)$ of the 1,4-PBD solutions can be determined by separately measuring the tube diameter $a$ and the reptation time $\tau_d$ as a function of $\phi$ at different temperatures. Both quantities have been evaluated for the solutions as shown in Figures 5, 7, and 9. Figure 10 demonstrates that the friction dynamics represented by $\zeta(\phi,T)$ can be rheologically obtained as a function of $\phi$ and $T$ in terms of $\zeta_0$ of the pure PBD without any need for labeled polymers and without invoking any hypothesis other than the validity of the reptation theory for linear viscoelasticity of entangled monodisperse solutions.

The temperature dependence of $\zeta(\phi,T)$ is to a first-order approximation related to the effective glass transition temperature $T_g(\phi)$ in a WLF fashion as shown in (3). In particular, we have

$$\log\left[\frac{\zeta(\phi,T)}{\zeta_0(T)}\right] = \log\left[\frac{\zeta_g(\phi)}{\zeta_{g0}}\right] + \frac{c_{10}(T - T_{g0})}{c_{20} + T - T_{g0}} - \frac{c_1[T - T_g(\phi)]}{c_2 + T - T_g(\phi)} \quad (8)$$

where the subscript zero denotes the case of pure polymer ($\phi = 1.0$). According to (4b), the WLF constants $c_1$ and $c_2$ for the solution appropriate to $T_g(\phi)$ can be obtained from the WLF constants $c_{01}$ and $c_{02}$ appropriate to the reference temperature $T_0$. Table 2 lists the reference temperatures and corresponding WLF constants as well as the $c_1$ and $c_2$ appropriate to $T_g(\phi)$.

Figure 11 shows that (8) can reasonably describe the temperature dependence of the segmental friction coefficient $\zeta(\phi,T)$ at different values of $\phi$. In fitting the experimental data with (8) using $T_g(\phi)$, $c_1$, and $c_2$ listed in Table 2, we adjust the calculated curves vertically and obtain the shifting factor as a function of $\phi$, which is the first term of (8). Thus, this procedure actually allows us to evaluate the friction coefficient $\zeta$ at the respective glass transition temperatures relative to that of the pure PBD1. We find in Figure 12 that $\zeta_g(\phi)$, denoted by the circles, varies by 2 orders of magnitude across the whole range of $\phi$. This is qualitatively consistent with the limiting values of $\zeta_g$ for the pure 1,4-PBD and 1,2-PBD listed in Table 12-III on p 330 of ref 13.

A second fitting represented by the thin lines in Figure 11 is made by freely adjusting $T_g(\phi)$ in (8) instead of using its values obtained from the DSC. Specifically, we find that the values of $T_g'$ listed in Table 2 give a much better fit as shown in Figure 11. The difference

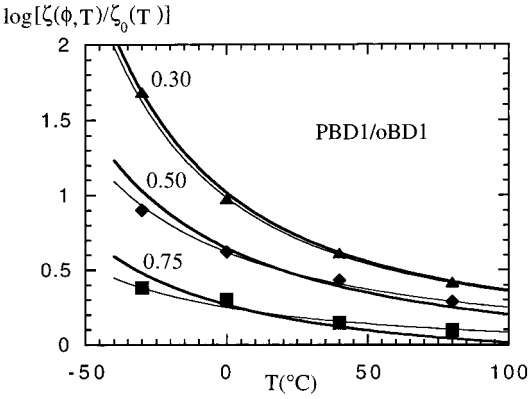


**Figure 11.** Temperature dependence of the segmental friction coefficient ratio $\zeta/\zeta_0$ as at different compositions, where the thick lines are predictions by (8) using $T_g(\phi)$ in Table 2 determined by DSC and the thin lines are obtained by freely adjusting $T_g$ in (8) to $T_g'$ listed in Table 2 to give the best fit.

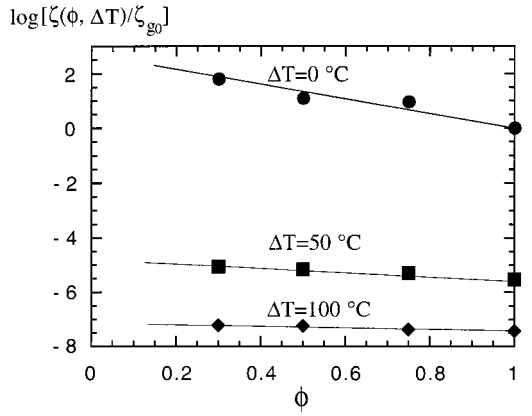


**Figure 12.** Reduced segmental friction coefficient $\zeta(\phi,\Delta T)/\zeta_{g0}$ of PBD1/oBD1 solutions at three fixed distances from the respective glass transition temperature $T_g(\phi)$ as a function of $\phi$, $\Delta T = 0$, 50, and 100 °C, where the data corresponding to $\Delta T = 0$ °C is obtained by vertically shifting the prediction (8) to fit the data in Figure 11.

between $T_g$ and $T_g'$ decreases with $\phi$. This represents a downward deviation from the actual $T_g$ given by DSC and hints at a self-plasticization effect. Any further elaboration of the implication is beyond the present scope and will be the focus of a future publication.

At any given temperature $T$, $\zeta(\phi,T)$ is larger for a lower $\phi$ as indicated in Figure 11 because the solution with lower $\phi$ is closer to its $T_g(\phi)$ given in Figure 8. The separation between the curves grows with lowering $T$. To view the segmental friction dynamics in a more instructive way, we evaluate $\zeta$ at an equal distance from the respective $T_g$ as determined from the DSC according to (3), where $c_1$ and $c_2$ are listed in Table 2, and the $\phi$ dependence of $\zeta_g(\phi)$. Besides $\zeta_g(\phi)$, Figure 12 shows $\zeta(\phi,\Delta T)$ as a function of $\phi$ at $\Delta T = T - T_g(\phi) = 50$ and 100 °C, respectively.[17] As expected, $\zeta(\phi,\Delta T)$ hardly varies with $\phi$ when the samples are set at an equal distance far away from their own $T_g(\phi)$. Specifically, $\zeta(\phi,\Delta T)$ at $\Delta T = 50$ °C decreases no more than a factor of 3 as $\phi$ increases from 0.3 to 1.0. The maximum variation occurs at the glass transition temperatures. More explicitly, using (3) we can describe $\zeta(\phi,\Delta T)$ at all values of $\Delta T$ as shown in Figure 13 for $\phi = 0.3$, 0.5, 0.75, and 1.0.

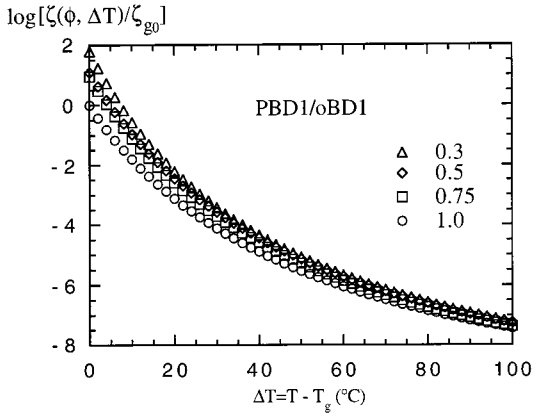


**Figure 13.** Reduced segmental friction coefficient $\zeta(\phi,\Delta T)/\zeta_{g0}$ of the four samples as a function of the equal distance $\Delta T$ from the respective $T_g$.

## Conclusions

Using a model solution, we are able to elucidate the power of a new experimental approach to explore component dynamics of polymer mixtures. The method is not limited to two-component systems and actually has the advantage to deal with any number of components. The entangled 1,4-PBD solutions selectively reveal the dynamics of 1,4-PBD in the presence of butadiene of high and low vinyl contents in a mean-field fashion. To the first-order approximation, the dynamic coupling between two species can be described by their effective glass transition temperature $T_g(\phi)$. Since the 1,4-PBD solutions have significantly higher $T_g(\phi)$ than $T_{g0} = -94$ °C of the pure 1,4-PBD, the polymer dynamics show considerable slowing down despite the dilution effect created by the oligomeric solvent oBD1. At approximately 40 °C, the PBD/oBD1 solutions have essentially an overall molecular relaxation time $\tau_d(\phi)$ that is independent of $\phi$, whereas their elastic plateau moduli $G_N^0(\phi)$ decrease remarkably with lowering $\phi$. This occurs because the increased segmental friction $\zeta$ is counterbalanced by the effect of tube dilation to keep $\tau_d(\phi)$ of (2) constant. Thus, we arrive at a unique series of polymer samples whose viscosity $\eta$ drops strongly as $G_N^0(\phi)$ plunges with lowering $\phi$ although the molecular relaxation time remains constant.

By exploiting the detailed description of the classical reptation theory for entangled polymers, we are also able to reveal the scaling behavior associated with the tube dilation, $a \propto \phi^{-2/3}$ and $G_N^0(\phi) \propto \phi^{7/3}$, throughout the composition range without invoking any sophisticated experimental techniques such as neutron scattering and spin echo measurements.[15] For monodisperse polymers, we expect these scaling laws to be universal as long as the solutions are sufficiently entangled.

The present work demonstrates that the segmental friction coefficient $\zeta$ of a polymer A can be evaluated at various compositions in a blend of A and B by studying entangled polymer A solutions in oligomeric B. The experimental results indicate that $\zeta(\phi,T)$ is a *monotonic* function of the composition $\phi$ at an equal distance $\Delta T = T - T_g(\phi)$ from the effective glass transition temperatures. It appears that the friction coefficient at the glass transition $\zeta_g(\phi)$ is larger for a higher $T_g(\phi)$ for these butadiene-based systems.

Since the friction dynamics of the 1,4-PBD solutions are considerably faster than those of the oligomeric butadiene of high vinyl content (oBD1) and change with

temperature less strongly, the observed dynamic behavior of these solutions reflect a plasticization effect. In other words, the 1,4-PBD significantly lowers the overall glass transition temperature of the solution in comparison to that of the pure oBD1 and causes accelerated chain dynamics relative to those dictated by oBD1. Nevertheless, the thick lines in Figure 11 show that the polymer dynamics are not so adequately depicted when using $T_g(\phi)$ obtained from DSC. It appears that the 1,4-PBD senses a lower effective glass transition temperature $T_g'(\phi) < T_g(\phi)$ which gives a more accurate description of the temperature dependence of $\zeta$ as shown in Figure 11. Such a possibility would be a self-plasticization effect that has not yet been fully explored in the literature although it may be the origin of breakdown of the time−temperature superposition in similar polymer blends.[2] More systematic studies need to be carried out to investigate the implication of such a self-plasticization phenomenon.

**Acknowledgment.** This work is supported by the National Science Foundation (Grant CTS-9632466).

## References and Notes

(1) Colby, R. H. *Polymer* **1989**, *30*, 1275.
(2) Roovers, J.; Toporowski, P. M. *Macromolecules* **1992**, *25*, 1096, 3454.
(3) Arendt, B. H.; Kannan, R. M.; Zewail, M.; Kornfield, J. A.; Smith, S. D. *Rheol. Acta* **1994**, *33*, 322.
(4) Composto, R. J.; Kramer, E. J.; White, D. M. *Polymer* **1990**, *31*, 2320.
(5) Green, P. F.; Adolf, D. B.; Gilliom, L. R. *Macromolecules* **1991**, *24*, 3377.
(6) Composto, R. J.; Kramer, E. J.; White, D. M. *Macromolecules* **1992**, *25*, 4167.
(7) Kim, E.; Kramer, E. J.; Osby, J. O. *Macromolecules* **1995**, *28*, 1979.
(8) Chapman, B. R.; Hamersky, M. W.; Milhaupt, J. M.; Kostelecky, C.; Lodge, T. P.; von Meerwall, E. D.; Smith, S. D. *Macromolecules* **1998**, *31*, 4562.
(9) Arendt, B. H.; Krishnamoorti, R.; Kornfield, J. A.; Smith, S. D. *Macromolecules* **1997**, *30*, 127.
(10) Doi, M.; Edwards, S. F. *The Theory of Polymer Dynamics*; Clarendon Press: Oxford, 1986.
(11) De Gennes, P. G. *J. Chem. Phys.* **1971**, *55*, 572.
(12) Graessley, W. W.; Edwards, S. F. *Polymer* **1981**, *22*, 2869.
(13) Ferry, J. D. *Viscoelastic Properties of Polymers*, 3rd ed.; Wiley: New York, 1980.
(14) Colby, R. H.; Rubinstein, M. *Macromolecules* **1990**, *23*, 2753.
(15) Richter, D.; Farago, B.; Butera, R.; Fetters, L. J.; Huang, J. S.; Ewen, B. *Macromolecules* **1993**, *26*, 795.
(16) Raju, V. R.; Menezes, E. V.; Marin, G.; Graessley, W. W.; Fetters, L. J.; *Macromolecules* **1981**, *14*, 1668.
(17) An alternative way to obtain such information as presented in Figure 12 would be to consider $\log[\zeta(\phi,T)/\zeta_{g0}] = \log[\zeta(\phi,T)/\zeta_0(T)] + \log[\zeta_0(T)/\zeta_{g0}]$, get the first term at fixed values of $\Delta T = T - T_g(\phi)$ by empirically fitting the data in Figure 11 with continuous curves and reading respective values of $\zeta$ at fixed $\Delta T$, and evaluate the second term according to (3) based on the measured values of $c_{10}$, $c_{20}$, and $T_g$ for the pure PBD. Such a description is independent of any knowledge about the $\phi$ dependence of $\zeta_g(\phi)$.

MA981778W